Multifarious Photoinduced Morphologies in Monomolecular Films of Azobenzene Side Chain Polymer on Mica

Takahiro Seki,* Jun-ya Kojima, and Kunihiro Ichimura

Photofunctional Chemistry Division, Research Laboratory of Resources Utilization, Tokyo Institute of Technology, 4259 Nagatsuta, Midori-ku, Yokohama 226-8503, Japan

Received August 24, 1999; Revised Manuscript Received January 26, 2000

ABSTRACT: Monomolecular films of a poly(vinyl alcohol) derivative having an azobenzene (Az) side chain (6Az10-PVA) transferred onto mica by the Langmuir−Blodgett technique were observed by atomic force microscopy in the noncontact mode. Multifarious features of the film morphology after the thermal and photostimulated processes were revealed, which were strongly dependent on the humidity of the atmosphere, the lateral packing density of the monolayer, and the light exposure dose. In a humidified atmosphere, a low-density film (1.2 nm^2 Az^{-1}) showed a network morphologythat exhibited a two-dimensional expansion upon irradiation with UV (365 nm) light (trans → cis Az isomerization). The films having the higher densities (0.4 or 0.3 nm^2 Az^{-1}) gave spongy-shaped or partially collapsed films and indicated a formation of three-dimensional protrusions on UV light illumination. In comparison with the spectroscopic data, these morphological changes could be related with the proceeding of the Az photoreaction. The morphological changes were basically reversible, however, and showed large deviations depending on the back (cis → trans) processes, i.e., thermally or photochemically with visible light (436 nm). In-situ tapping mode observations of 6Az10-PVA monolayer on mica in water were further performed. The monolayers immersed in water showed completely different photoinduced deformations with no reversibility.

1. Introduction

In the past two decades, much attention has been paid to light-stimulated mechanical effects observed in photochromic monomolecular films (monolayers) on a water surface.[1−9] In the monolayer systems, molecular motions taking place in the each photochromic unit may be accumulated to show the macroscopic response in the two dimensions. This situation allows precise understandings of the molecular motility of photoresponsive materials.

Our current work has been devoted to the observation of photoinduced area changes of monolayers consisting of a poly(vinyl alcohol) bearing an azobenzene unit in the side chain (6Az10-PVA, Figure 1) on water. The trans-to-cis photoisomerization of Az upon UV (365 nm) light irradiation leads to a large increase in the dipole moment of this unit,[10] and this part gains a high affinity to a water surface. This gives rise to an expansion of the molecular film at low pressures.[7,8] On visible light (436 nm) irradiation, the reverse process takes place, and the alternate irradiation results in the expansion and contraction with full reproducibility. The validity of the molecular model mentioned above have been strongly supported by the surface pressure−area isotherm,[7,8] surface potential,[11] and X-ray reflectivity[12] measurements.

Microscopic observations are found to be of particular use to gain essential understandings of the photoresponse behavior of monolayers. Brewster angle microscopic (BAM) measurement having a resolution of a few micrometers provided a great deal of information on the morphological and rheological features induced by illumination[13] and revealed a strong molecular cooperativity involved in the photomechanical response on the water surface.[11,14] On the other hand, our preliminary work also revealed that the monolayer of 6Az10-PVA exhibits large photoinduced morphological changes on a mica surface in a humidified atmospheres.[15] The hydration on the surface should play an important role in the film motility on the solid surface (see illustration in Figure 1). Since AFM provides morphological information from micrometers down to the molecular level, it is anticipated that more in-depth interpretation and clarification of the molecular mechanism are available by this method.[16] A closely related phenomenon on the morphological photoinduction in Az-containing polyion complex type LB films on mica has also been investigated by Matsumoto and co-workers.[17] In their work, the experiments are carried out at ambient atmosphere, and atmospheric factors such as the humidity and light exposure energy had not been considered.

In the above contexts, this paper describes our detailed explorations on the photostimulated morphological changes in the 6Az10-PVA monolayer on mica. The aspects such as effects of humidity, lateral density of the Az unit, and light exposure dose on the film morphologies are presented. This report also includes the results obtained by the in-situ tapping mode AFM observations of this monolayer on mica immersed in water, which can be regarded as the extreme condition of the hydration state.

2. Experimental Section

2.1. Materials. The synthesis of 6Az10-PVA was described previously.[18] Chloroform for monolayer spreading was of UV spectroscopic grade (Uvasol, Ciba-Merck). Mica was of C&SS (clear and slightly stained) grade and was purchased from Watanabe Shoko Co.

2.2. Methods and Characterizations. All procedures were carried out in dimmed red light at 20 ± 1 °C.

Light irradiation was performed with a 150 W Hg−Xe lamp (San-ei UV Supercure-203S) equipped with an optical fiber

* To whom correspondence should be addressed. Fax +81-45-924-5247, e-mail tseki@res.titech.ac.jp.

10.1021/ma991439i CCC: $19.00
Published on Web 03/17/2000

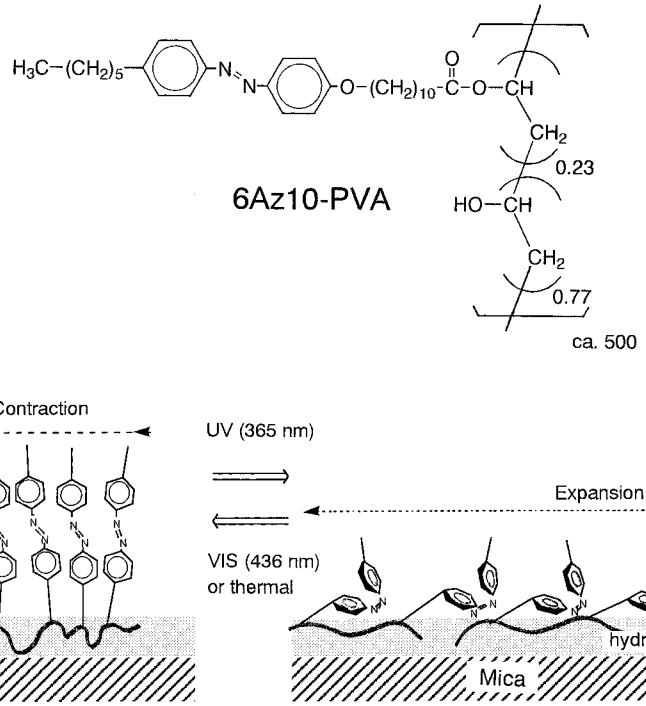

Figure 1. Structure of 6Az10-PVA and plausible molecular mechanism for the water-assisted photoresponsive behavior of this monolayer.

which favors irradiation to a target part. The 356 nm (UV) and 436 nm (visible) lines from the lamp were selected passing through combinations of Toshiba optical filters, UV-35/UV-D36A and Y-44/V-42, respectively. Light intensity was evaluated with an optical power meter (Advantest TQ-8210). The light power was adjusted to 1.0 mW cm^{-2} for both 365 and 436 nm lines.

The monolayer of 6Az10-PVA was spread from a chloroform solution (1.0×10^{-3} mol dm^{-3}) on pure water (Milli-Q grade, 18 MΩ cm^{-1}) filled on a Lauda FW2 film balance. The spread film was compressed at a speed of 30 cm^2 min^{-1}. The chloroform solution was preirradiated with UV or visible light before spreading, which was effective for homogeneous film formation and an area control in a wide range (see section 3.1). A freshly cleaved mica of 20×10 mm^2 in size was first immersed into water, and then the 6Az10-PVA monolayer was spread onto the water surface. The monolayer was transferred onto mica by the upstroke vertical lifting at a speed of 0.2 mm min^{-1}. These mica plates were attached onto a glass slide with an adhesion tape for AFM measurements.

Control of relative humidity (RH) was attained in a sealed vessel wherein a proper saturated salt aqueous solution was present [$NaClO_3$ (ca. 80%), $NaHSO_4$ (60%), and $CaCl_2$ (ca. 40%)]. The dry atmosphere (RH ≤ 25%) was supplied in the presence of drying silica gel beads.

UV−vis absorption spectrum measurements were carried out on a JASCO MAC-1 spectrometer at ambient atmosphere.

AFM measurements in air atmosphere were conducted in the noncontact dynamic force mode with a Seiko Instruments SPA300/SPI3700 system. A microcantilever of SI-DF20 (20 μm scanner, a rectangular-shaped Si tip) was used. The radius of the tip terminus was 10−15 nm, and a spring constant was 11 N/m according to the manufacturer. The scanning speed was 2.0−4.1 Hz. The contact mode AFM measurement was carried out with a microcantilever of SN-AF01 (Si_3N_4 tip). Measurements were performed at ambient atmosphere at RH below 40%. In general, the contact mode AFM observation of the monolayer films used in this study was destructive. Scratched and damaged traces in the direction of cantilever scans were observed for the 6Az10-PVA monolayers particularly in the *cis*-Az state. However, the *trans*-6Az10-PVA monolayer in a dried state was robust enough for the contact mode measurements. The film thickness of 6Az10-PVA was measured in both the contact and noncontact modes. The thickness of a film (A_{oc} (given area per Az) = 0.4 nm^2 Az^{-1}, see below) evaluated in the contact and noncontact mode was 2.6 ± 0.1 and 2.4 ± 0.1 nm, respectively. Essentially the same values were obtained, indicating that the height profiles observed in the noncontact mode were sufficiently accurate. Therefore, all images were taken in the noncontact mode.

The tapping mode AFM measurements in water was carried out with an Olympus NVB100 (AFM system, Nanoscope III, Digital Instruments) which is most suited for biological soft specimens in aqueous solutions. In this microscopic system, in-situ monochromatic light irradiation can be achieved with a ready-equipped Xe lamp (100 W) through optical filters. This light source is routinely used for light excitation of fluorescence imaging. The height profile was calibrated by measuring of the standard crystal step of Si(111) (0.35 ± 0.03 nm).[19]

3. Results and Discussion

3.1. Film Deposition onto Mica. The surface pressure−area isotherms of 6Az10-PVA monolayer on pure water in the *trans*- and *cis*-Az at 20 °C are already reported previously (see, e.g., Figure 1 of ref 13). We have selected three area conditions for deposition onto mica, the occupying areas per Az unit (A_{oc}) being 1.2, 0.4, and 0.3 nm^2 Az^{-1}. The most sparse (A_{oc} = 1.2 nm^2 Az^{-1}) and the medium (A_{oc} = 0.4 nm^2 Az^{-1}) films were prepared from the highly expanded *cis*-6Az10-PVA monolayer[13] which was preirradiated with UV light before spreading. The most dense film (A_{oc} = 0.3 nm^2 Az^{-1}) was transferred from the *trans*-6Az10-PVA monolayer. Also in this monolayer, 10% of cis isomers were involved by irradiation with 436 nm light for successful and homogeneous deposition. The corresponding surface pressures of deposition for the films of A_{oc} = 1.2, 0.4, and 0.3 nm^2 Az^{-1} were 2, 13, and 30 mN m^{-1}, respectively.

3.2. UV−vis Absorption Spectroscopy. Spectral changes of the 6Az10-PVA monolayer upon illumination were directly observed on the mica surface. Since it was difficult to evaluate the background absorption of mica for the monolayer sample, the photoreaction was monitored in the difference spectra, in which the spectra of

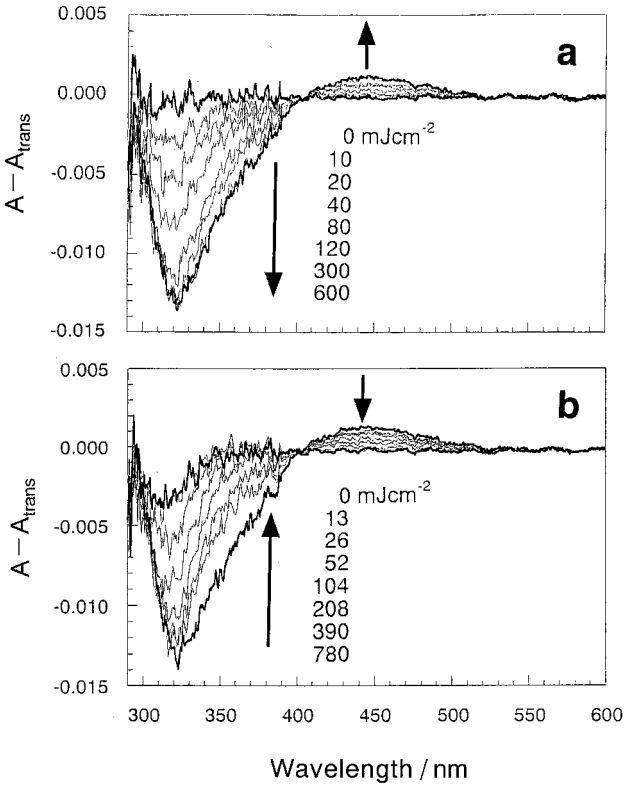

Figure 2. UV−vis absorption difference spectra of 6Az10-PVA monolayer on mica at A_{oc} = 0.4 nm^2 Az^{-1} on the processes of UV light (a) and successive visible light (b) illumination. The spectra at each stage were subtracted from that of the initial *trans*-Az state.

irradiated films were subtracted from that of the initial *trans*-Az state. The difference spectra so obtained are indicated in Figure 2 for the film of A_{oc} = 0.4 nm^2 Az^{-1} as an example. The irradiation with 365 nm light brought about a depression in the spectra in the wavelength region below 400 nm (corresponding to the $\pi-\pi^*$ transition) and a rise in the region of 400−500 nm (n−π^*) (a). These changes show the features of the trans-to-cis photoisomerization of the Az unit. The reaction reached to the photostationary state at an exposure energy of 150−200 mJ cm^{-2}.

The reverse changes were observed upon irradiation with 436 nm light (b). The photostationary state in this case was attained within 400 mJ cm^{-2}. The spectrum at the final stage did not completely revert to the initial horizontal baseline, indicating a partial involvement of the cis isomers.

The light energy required for the photoequilibration was essentially invariable by the change in the density of Az unit and humidity conditions.

3.3. Morphological Observation by AFM. 3.3.1. Thermal Film Contractions at Various Humidities. AFM topographies showed that the surface of the fresh monolayer films within 30 min after deposition for A_{oc} = 1.2 and 0.4 nm^2 Az^{-1} were defect-free and molecularly smooth with a roughness below 1 nm.

These films were stored in the dark at room temperature for 4−7 days in humidified atmospheres. The film exhibited completely different morphologies after dark adaptation. As stated in the section 3.1, the transfer of these films was carried out in the cis-rich state (ca. 90% cis content). The full thermal reversion to the trans form of Az was completed in 4 days as evaluated by UV−vis absorption spectroscopy. It is reasonable to assume that the morphological change, i.e., contraction of the monolayer, is associated with this thermal process (denoted as "thermal" in Figure 1).

The morphologies of the sparse monolayer (A_{oc} = 1.2 nm^2 Az^{-1}) after 7 days were observed at various humidities (Figure 3). For the films stored at RH exceeding 40% (a−c), the morphology considerably changed depending on the humidity. The more humid condition gave rise to the lateral film contraction in larger scales. At RH = 40% (c), split open round gulfs below 1 μm in diameter were observed, seemingly as a result of incomplete lateral movement. On the other hand, complete shrinkage performed at RH exceeding 60% yielded network morphologies (a and b). The more humid condition led to the larger scale of the network structure. In a dry state (RH = 25%), in contrast, a complete flat film that preserved the initial state was observed (d). The humidity dependence observed here undoubtedly shows that the hydration of the monolayer on mica[20] plays a critical role in the lateral migration of the film material. Under all these conditions, the film thickness were maintained below 2−3 nm, indicating that the lateral motions proceeded with retention of the two-dimensional monolayer state.

Chen and Israelachivili[21] described based on the surface force measurements that the hydration on mica will influence the above-layered monolayer in the following manners: (i) the monolayer is lifted from the mica surface to gain the overall thickness, (ii) the hydration layer reduces the monolayer-substrate adhesion, and (iii) the hydrated headgroup becomes able to move father apart laterally. The hydration on mica would provide a similar environment as on water for the 6Az10-PVA monolayer. Self-contraction of the 6Az10-PVA monolayer on water in the course of the cis-to-trans photoisomerization is actually observed by BAM.[11] Essentially the same process should be occurring on hydrated mica. In a dry atmosphere, in contrast, the headgroup of the monolayer strongly adhered to the mica surface through dipole−dipole interaction and hydrogen bonding, and no lateral motion is attained irrespective of the cis-to-trans isomerization of the Az unit.

Importance of hydration in the mobility of the monolayer of amphiphilic molecules on mica has been demonstrated for single- and double-chain ammonium salts and a biological lipid.[22,23] In regard to polymer chain motility, extensions of poly(methyl methacrylate) chains on mica under humidified conditions was directly visualized by AFM.[24]

UV−vis absorption spectroscopy gave additional information on the thermal contraction process (data not shown here). The 6Az10-PVA monolayer on a quartz plate stored in a dry state for 1 week gave the absorption peak at 350 nm (the long axis $\pi-\pi^*$ band of Az) as observed in solutions. In contrast, a hypsochromic shift with an absorption maximum at 340 nm was observed for the network films that were stored at a high humidity. This blue shift for the hydrated film can be ascribed to the formation of H-type aggregation.[25] Thus, the film shrinkage to the network structure gives rise to the packing of the side chains to the level where the electronic state of Az unit is influenced.

3.3.2. Photoinduced Morphologies in Humidified Atmospheres. Figures 4, 5, and 6 show the UV light induced morphological changes of 6Az10-PVA monolayers of A_{oc} = 1.2, 0.4, and 0.3 nm^2 Az^{-1}, respectively,

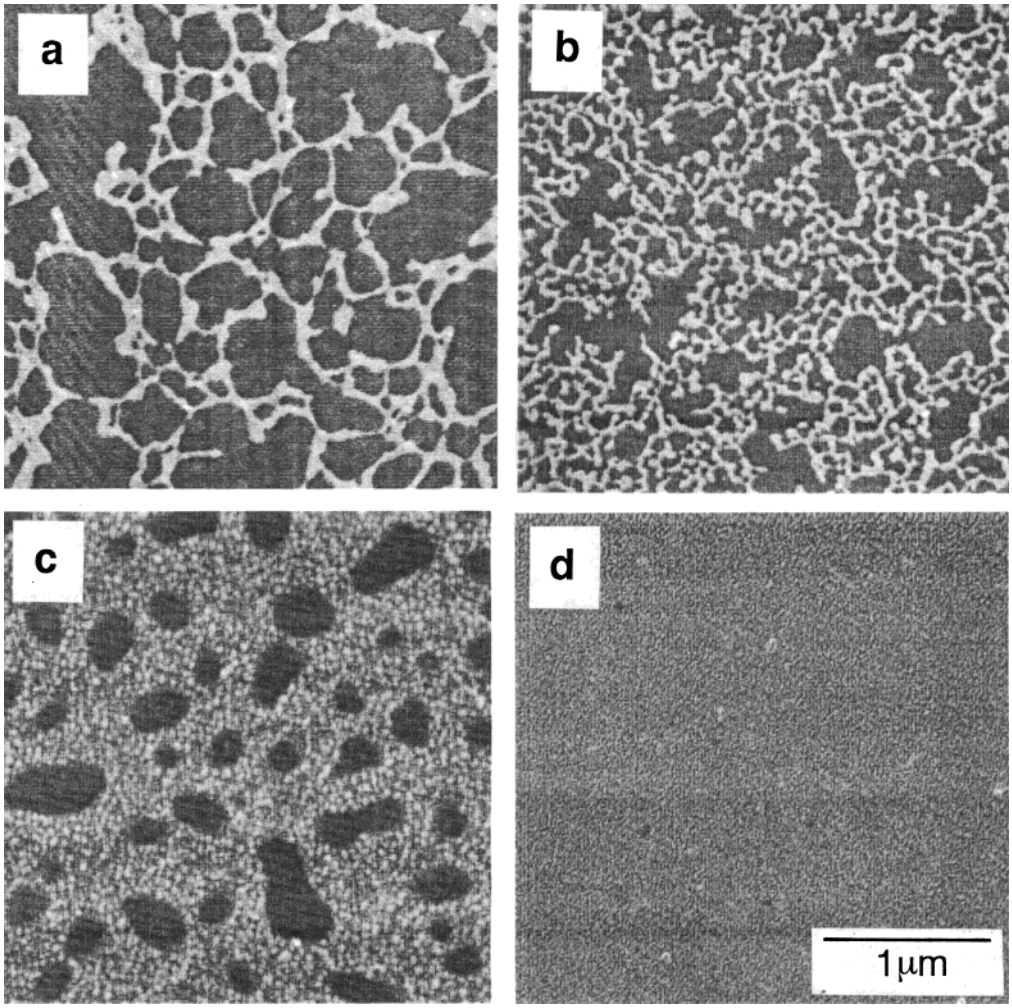

Figure 3. Topographical AFM images of 6Az10-PVA monolayers on mica at $A_{oc} = 1.2$ nm^2 Az^{-1} after dark adaptation at room temperature for 1 week under various humidity conditions. Relative humidities were above 80% (a), ca. 60% (b), ca. 40% (c), and below 25% (d). The monolayer was transferred in the *cis*-Az form and kept in the dark for 1 week, which allowed the complete thermal isomerization from the cis to trans form of Az (the back process in Figure 1). The most dark areas correspond to the bare mica surface. The film thickness were ca. 2 nm for all cases.

starting from the thermally reverted state at ca. 80% RH. In each series, the photoirradiation was performed on the mounting stage of the AFM module, and the images were taken at the identical position.

For the network film obtained at $A_{oc} = 1.2$ nm^2 Az^{-1} (Figure 4a), UV light irradiation immediately induced an expansion of the film. The expansion ceased at an exposure dose of 120 mJ cm^{-2}, which corresponds to that required to reach the photoequilibrium state. No appreciable change was perceived upon further illumination at the dose of 480 mJ cm^{-1} (b). The film thickness was reduced by ca. 1 nm through the film expansion from 2.4 ± 0.1 (initial) nm to 1.1 ± 0.1 nm (after exposure).

The dark adaptation in a humidified atmosphere for the film of $A_{oc} = 0.4$ nm^2 Az^{-1} gave spongy-shaped morphology with a number of defects (Figure 5a). The film thickness was 2.1 ± 0.1 nm. Upon UV light irradiation at the dose within the photostationary state (160 mJ cm^{-2}), smaller defects were filled in to yield a more smooth film (b). Further exposure (340 mJ cm^{-2}) led to a three-dimensional modification, namely an appearance of many protrusions having ca. 100 nm in diameter (undeconvoluted for the tip width) and 2−3 nm in height (c).

The most dense film at $A_{oc} = 0.3$ nm^2 Az^{-1} at the initial state did not have defects but already possessed small projections of collapse with 1−2 nm height (Figure 6a). Unlike other films, illumination at 120 mJ cm^{-2} dose did not effect any changes in the film morphology. Appreciable changes were observed at 480 mJ cm^{-2}, an exposure dose far exceeding the photostationary state. Many larger protrusions with the diameter of 100−300 nm and the height of 7 ± 2 nm appeared (b).

Figure 7 summarizes the features of the morphological changes as a function of UV light exposure energy. The figure involves the light-induced changes of the monolayer coverage (percent) (a), film thickness (b), and height of the light-induced three-dimensional protrusion (c). The film coverage was evaluated by the NIH image processing. Areas of the film were calculated with a 20% threshold of the highest level in the AFM image to exclude the noise signal. The hatched part corresponds to the regime where the photoisomerization of Az proceeds to reach the photostationary state based on the data of Figure 2. The followings can be deduced. First, the 2D morphological changes, as seen from the changes of the monolayer coverage and thickness variations (a and b), are attained within the doses of the photoequilibration. Second, the 3D protrusion formation is starts at exposures beyond the photostationary state (c). Thus,

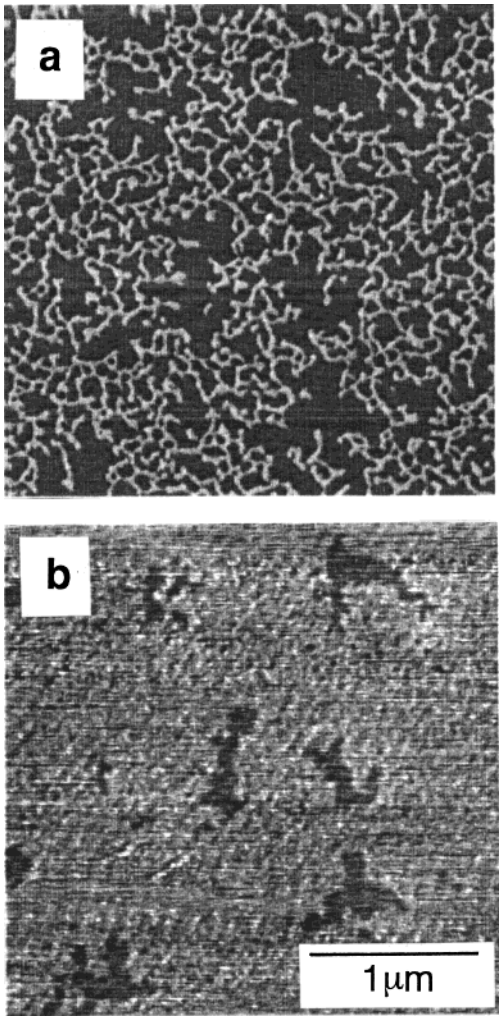

Figure 4. Topographical AFM images of the 6Az10-PVA monolayer on mica at $A_{oc} = 1.2$ nm^2 Az^{-1} before (a) and after UV light irradiation at 480 (b, 480 s) at RH = 80%. Essentially the same image as (b) was already obtained with irradiation at 120 mJ cm^{-2} (120 s). The film thickness in (a) and (b) were 2.4 ± 0.1 and 1.1 ± 0.1 nm, respectively.

the 2D motional process is almost in accord with the proceeding of the photoisomerization, and the 3D motion is a delayed process achieved after the completion of the 2D expansion.

The height versus diameter of randomly selected photoinduced 3D protrusions in Figure 6b was plotted to gain insight into the 3D structure formation (Figure 8). Two explanations would be possible for the formation of the 3D protrusions, namely, a film collapse to form multilayers and a bubble formation resulting from the film distortion. If the former is the case, the height values should be settled in the integral multiples of the monolayer thickness irrespective of the diameter. However, the height values observed were scattered and proportional to the diameter, and the extrapolation line comes to the zero point of the two axes. This strongly suggests that the bubble formation is more plausible for the mechanism of the 3D structuring. The bubble formation is probably the consequence of an excess lateral pressure after the defect coverage.

3.3.3. Photoinduced Segregation. The above UV light-induced morphologies were essentially reverted to the original ones when films were stored in the dark for 4 days at high RH exceeding 80%.[15] On the other hand, the photoreversion from to the *trans*-Az with 436 nm light provided a completely different shape of the film (Figure 9). The network film at $A_{oc} = 1.2$ nm^2 Az^{-1} (a) showed an expansion upon UV light irradiation (b, expansion was not complete in this case). The successive photoirradiation with 436 nm light produced even-sized dot films (c). The images (b) and (c) were reproducible on the alternate illumination of UV and visible light. Thus, for the cis-to-trans back-reaction, the thermal

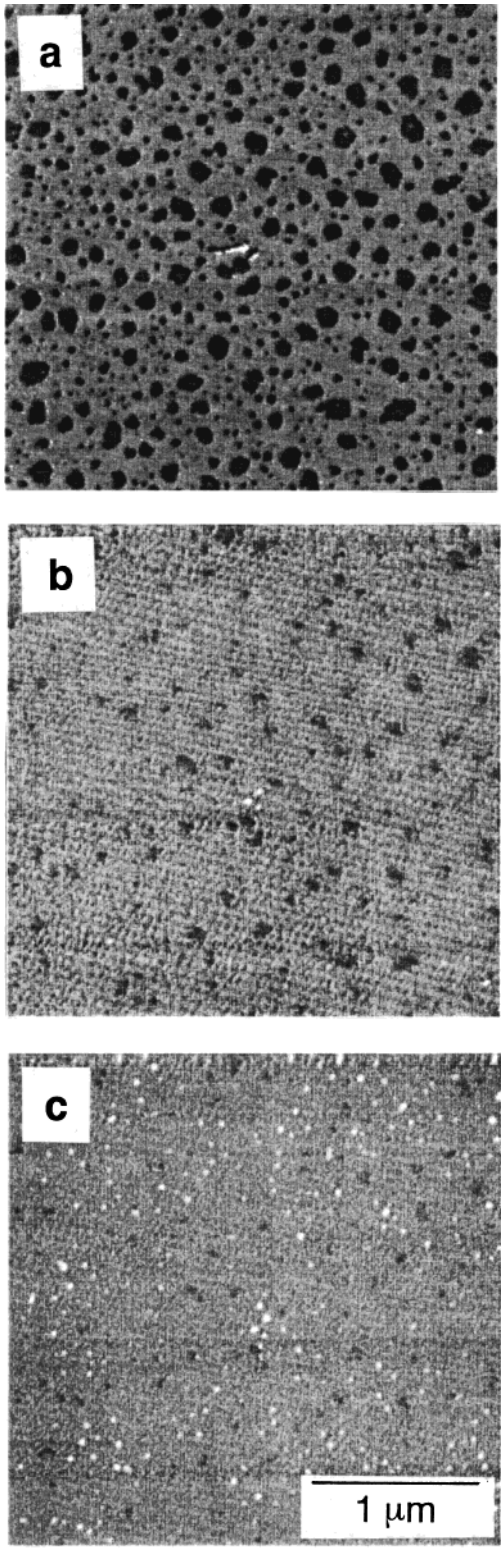

Figure 5. Topographical AFM images of the 6Az10-PVA monolayer on mica at $A_{oc} = 0.4$ nm^2 Az^{-1} before (a) and after UV light irradiation at 160 (b, 160 s) and 340 mJ cm^{-2} (c, 340 s) at RH = 80%. For the height profiles of these films, see text.

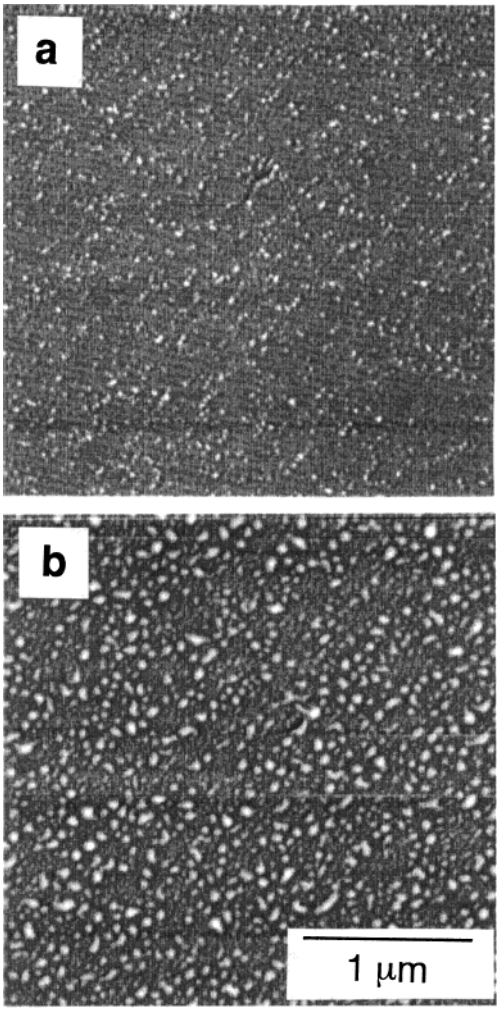

Figure 6. Topographical AFM images of the 6Az10-PVA monolayer on mica at $A_{oc} = 0.3$ nm^2 Az^{-1} before (a) and after UV light irradiation at 480 mJ cm^{-2} (b, 480 s) at RH = 80%. No change was admitted with the irradiation at 160 mJ cm^{-2} (160 s). For the height profiles of these films, see text.

processes and photoprocesses led to completely different morphologies. The following explanations would be possible. The fast photoisomerization process that ceases in minutes allows only a local film contraction, leading to the dot formation. Through the slow thermal process spending for days, on the other hand, the migration of the monolayer in the submicrometer scale becomes possible; thereby the original network structure can be reproduced.[15]

The dot films observed in (c) probably consist of a single polymer chain of 6Az10-PVA in consideration of the dot size.[26] The average volume of the dot film was estimated to be 4.6×10^2 nm^3 with an assumption that the film has a cylindrical shape and with a lateral size correction by the transmission electron microscope. On the other hand, one polymer particle of 6Az10-PVA ($M_w = 1.0 \times 10^5$) should occupy a volume of 1.7×10^3 nm^3 assuming a tentative film density of 1.0 g cm^{-3}. We suppose that this coincidence is satisfactory taking into account the undeterminable quantities concerning the film density and geometry. The method for complete separation of these dot films and their photoresponse behavior was reported elsewhere.[26]

Also in the thermal contraction process, the dot formation, although incompletely, can be recognized under relatively low-humidity conditions as seen in Figure 3c for RH = 40%. The lateral migrating motion, in this case, should be more suppressed due to a less degree of hydration on mica. This will cause limited local

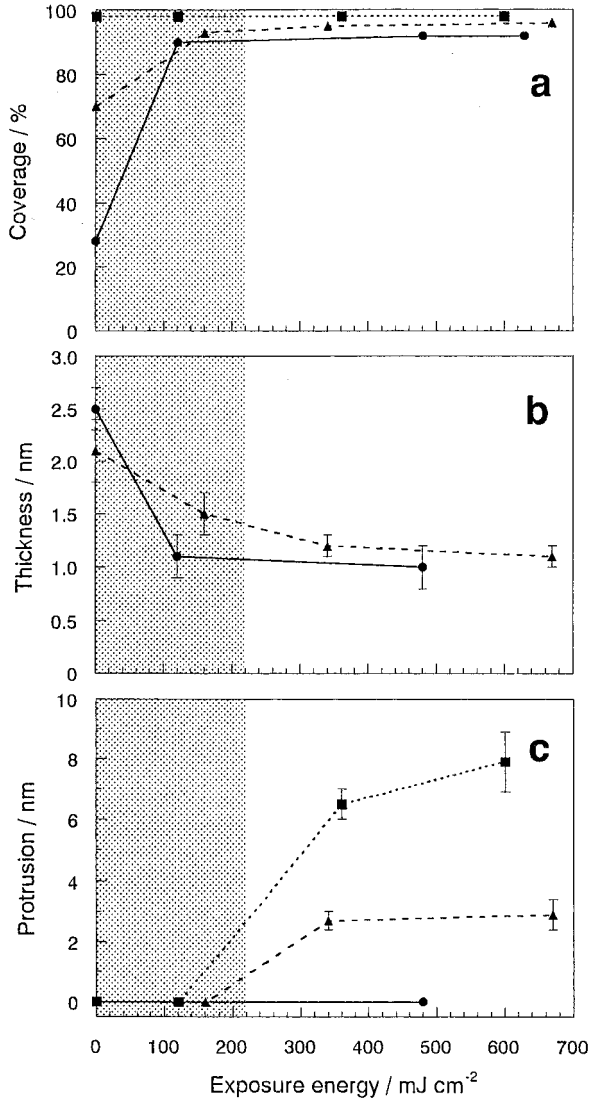

Figure 7. Changes in morphological features of 6Az10-PVA monolayer on mica in response to UV light illumination. Film coverage (a), film thickness (b), and height of protrusions (c) versus light exposure dose. Coverage of the monolayer film was evaluated by the NIH image processing program. Film thickness and height of protrusion were estimated by the AFM data of 10 randomly selected positions. The hatched part corresponds to the regime before reaching the photostationary state of Az.

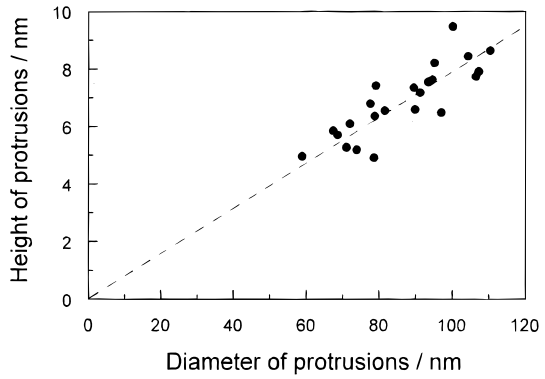

Figure 8. Height of randomly selected photoinduced protrusions versus their diameter taken from the data in Figure 6b.

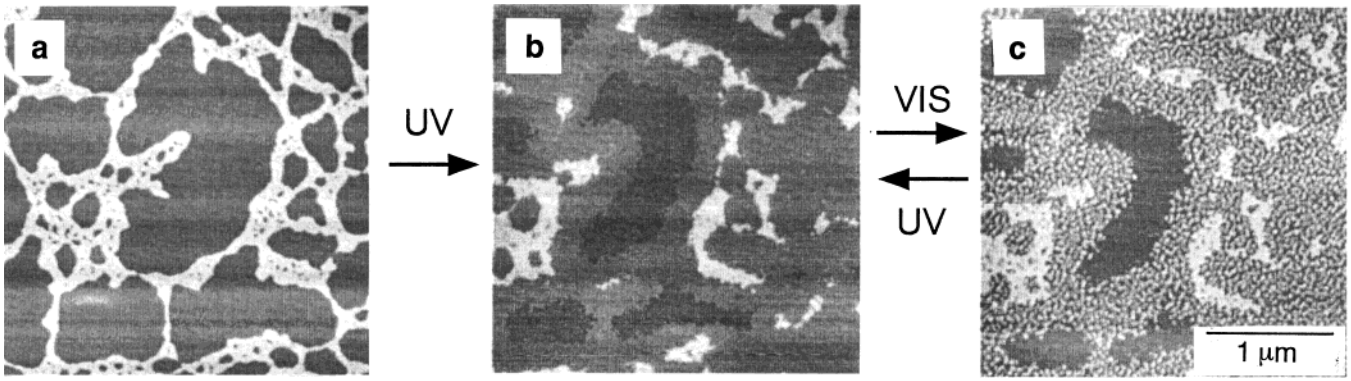

Figure 9. Morphological changes of 6Az10-PVA monolayer at A_{oc} = 1.2 nm^2 Az^{-1} after the UV→vis photocycle at RH = 80%. Initial state (a), after irradiation with 365 nm light (b), and after successive irradiation with 436 nm light (c). The states of (b) and (c) were reproducible after photocycles.

migrations as observed for the photoprocess. These facts should indicate that the resulting morphology after the contraction, i.e., either the network or dot structure, is governed by the lateral migration mobility given in the monolayer. When the migration rate of the monolayer is faster than the cis-to-trans isomerization, the lateral movement at a submicrometer scale will be possible, resulting in a network morphology. On the other hand, the segregation to dot film will be observed in the case that the lateral migration cannot overtake sufficiently the isomerization rate.

3.3.4. Illumination in a Dry State. Identical procedures were undertaken also for the films at A_{oc} = 0.4 and 1.2 nm^2 Az^{-1} in a dry atmosphere (RH = 30−40%). As expected, these films did not show any photoinduced morphological changes with irradiation of UV light at 300−500 mJ cm^{-2} (see Supporting Information).

On the other hand, the most dense film (A_{oc} = 0.3 nm^2 Az^{-1}) indicated some morphological changes upon UV light illumination in the dry atmosphere (see Supporting Information). Photogenerated protrusions obviously increased as shown in Figure 7a. The height of the protrusions was enhanced by 1.5 times on UV light illumination with retention of the number at the photostationary state (150 mJ cm^{-2}). Further illumination (540 mJ cm^{-2}) brought about an increase of the protrusion almost to the double in number.

The heights of protrusions were ca. 4 nm, which were lower than that obtained in the humid atmosphere (ca. 7 nm). Matsumoto et al.[17] also observed the reversible photoinduced protrusion formation in polyion complex type Az containing LB films at ambient atmosphere. In their LB film, the transfer was carried out at 25 mN m^{-1} from the monolayer in the *trans*-Az state. These conditions are very similar to that adopted for the most dense film of 6Az10-PVA (30 mN m^{-1}) under investigation. Height of protrusions of Matsumoto's monolayer is ca. 5 nm with a diameter of ca. 100 nm in their film. Thus, the morphological features of their film are very similar to ours.

We suppose that densely packed LB films consisting of Az side chain polymers, regardless of the side chain junction type (covalent or ion-complexed), commonly show 3D deformation to release the pressure arisen from the volume increase of the Az unit by the trans-to-cis photoisomerization. Thus, the 3D protrusion formation occurs for the densely packed LB films regardless of the humidity conditions. Humidity only affects the magnitude of the deformation.

3.4. In-Situ AFM Observation in Water. Figure 10 shows the images obtained by the in-situ AFM tapping mode measurements for the films of A_{oc} = 1.2 (a and b) and 0.4 nm^2 Az^{-1} (c and d). The film morphologies before irradiation (a and c) were essentially the same as obtained in the air atmosphere (cf. Figures 4a and 5a). However, the height difference between the mica surface and the film top was estimated to be 10−15 nm, ca. 5 times thicker than the monolayer thickness observed in air. This does not indicate a damage of the monolayer structure since subsequent drying of these samples gave identical images as shown in Figures 4a and 5a with a thickness ca. 2 nm. The height profile itself was sufficiently accurate as confirmed by the calibration as described in the Experimental Section. The overestimated thickness is attributable to swelling of the monolayer, participation of water (e.g., cluster formation on the hydrophobic surface monolayer[27−29]), and experimental artifacts. We are not yet able to figure out the origin of the large thickness observed in water. At least, immersion into water without irradiation does not damage the monolayer since a redried film exhibited exactly the same morphology of the original state.

UV light irradiation led to large morphological deformations that were entirely different from those observed in air. For the network film at A_{oc} = 1.2 nm^2 Az^{-1} (a), 2D expansion was hardly observed, but the film showed 3D projections to form dot structure with ca. 20 nm height (b). These protrusions showed some deformations due to the drag of the AFM cantilever (horizontal direction in the figure), probably indicating the elastic nature of the *cis*-Az film. The spongy-shaped film at A_{oc} = 0.4 nm^2 Az^{-1} also exhibited 3D structure formation providing larger droplet structures with ca. 40−60 nm height. These UV light-generated morphologies did not change any more with visible light irradiation. The morphological photoresponding process in water was irreversible. It seems that the film showed large 3D swelling with water due to increased polarity of the Az unit in the cis form. AFM observations in water imply that in air the strong adhesion to the mica surface through the capillary force plays an important role in the achievement of 2D and reversible deformation of the monolayer.

4. Conclusion

As described above, this work presents multifarious natures of thermally and photoinduced morphological changes in monolayers of the amphiphilic polymer having an Az side chain on mica. Intensive morphological investigations by AFM together with the spectroscopic data provided proper answers to the previous

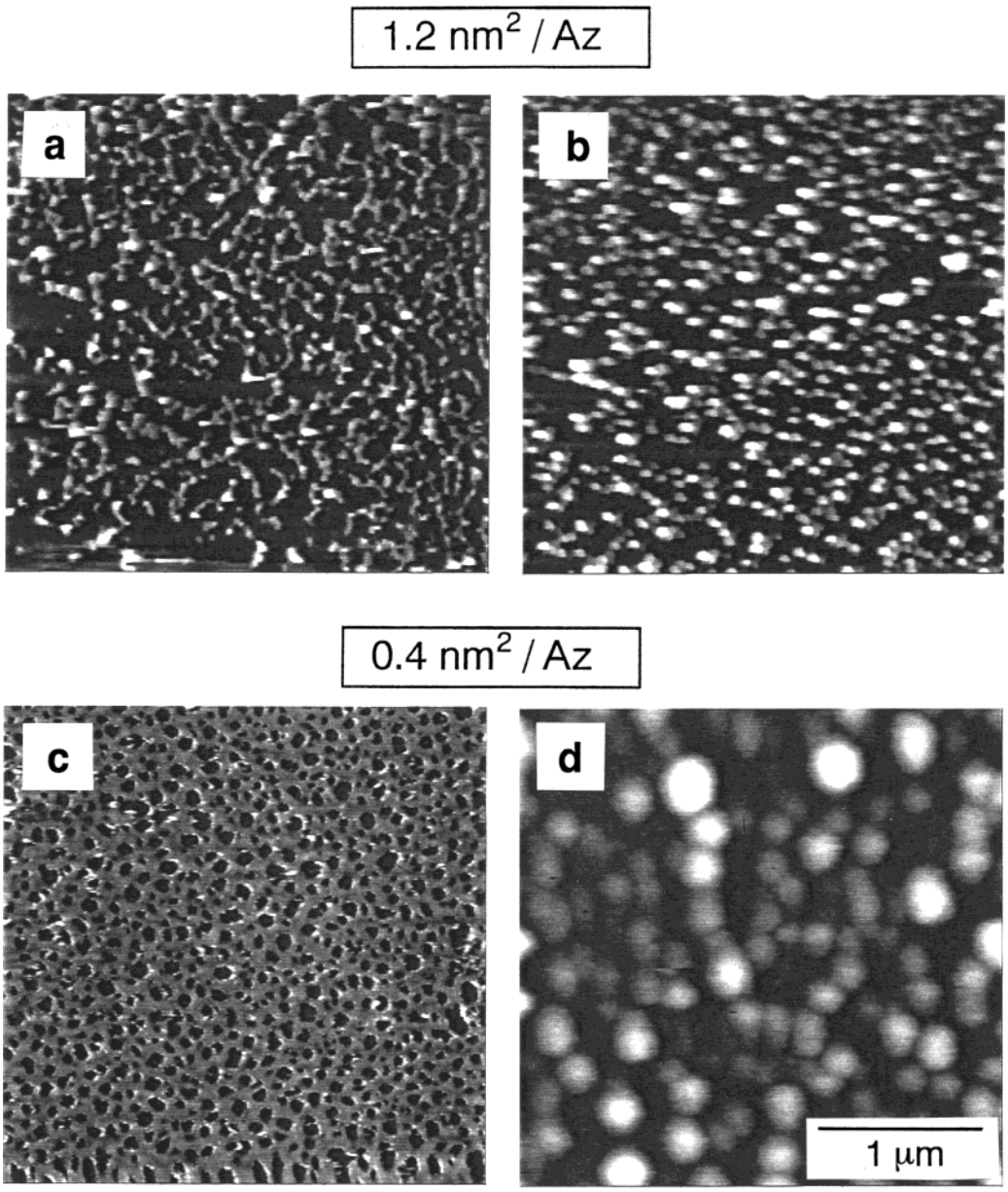

Figure 10. In-situ observation of the tapping mode AFM in water for 6Az10-PVA monolayer on mica at $A_{oc} = 1.2$ (a and b) and 0.4 nm^2 Az^{-1} (c and d) . Before (a and c) and after (b and d) UV light illumination.

pending questions[15,17] concerning the effects of the humidity variations, packing density of Az unit, and light exposure energy. The importance of hydration layer for the achievements of large photoinduced morphological changes in the 2D motions on mica is clearly indicated here. The photoinduced morphologies were successfully related to the photoisomerization proceeding in the both cases of the 2D and 3D processes.

It is worth pointing out that the most densely packed monolayer shows 3D photoinduced morphological changes even in a dry state, which is in agreement with Matsumoto's observation. On the other hand, laser beam induced holographic surface grating formation has become a subject of intensive research.[30−33] In such systems, high power interference irradiation with a laser beam onto thicker cast films of Az-containing polymers shows lateral mass migration of the polymer to form 3D surface relief gratings. The same principle has recently been applied also in LB multilayer systems.[33] Whether the surface grating formation and the light-driven morphological changes of monolayer observed in the present work are driven in the common mechanism or not is unclear and an alluring subject to be pursued in the future investigations.

Acknowledgment. We thank Mr. E. Imai and Mr. Yagi of Olympus Optics Cooperation for tapping mode AFM measurements in water and helpful discussions. We also thank Mr. S. Morino, Dr. M. Nakagawa, and Mr. Arimitsu for helpful discussions. This work was in part supported by the Grant-in-Aid for Scientific Research on Priority Areas, "New Polymers and Their Nano-Organized Systems (277/10126218)", from the Ministry of Education, Science, Sports and Culture.

Supporting Information Available: Supplementary AFM images for Figures 4 and 6 and AFM topographical images observed in a dry state described in section 3.3.4. This material is available free of charge via the Internet at http://pubs.acs.org.

References and Notes

(1) Polymeropoulos, E. E.; Möbius, D. *Ber. Bunsen-Ges. Phys. Chem.* **1979**, *83*, 1215.

(2) (a) Gruder, H.; Vilanove, R.; Rondelez, F. *Phys. Rev. Lett.* **1980**, *44*, 590. (b) Vilanove, R.; Hervet, H.; Gruder, H.; Rondelez, F. *Macromolecules* **1983**, *16*, 845. (c) Panaiotov, I.; Taneva, S.; Bois, A.; Rondelez, F. *Macromolecules* **1991**, *24*, 845.
(3) (a) Blair, H. S.; Pogue, H. I. *Polymer* **1976**, *20*, 55. (b) Blair, H. S.; Pogue, H. I.; Riordan, J. E. *Polymer* **1980**, *21*, 1195. (c) Blair, H. S.; McArdle, B. *Polymer* **1984**, *25*, 1347.
(4) Malcolm, B. R.; Pieroni, O. *Biopolymers* **1990**, *29*, 1121.
(5) Menzel, H. *Macromol. Chem. Phys.* **1994**, *195*, 3747.
(6) Higuchi, M.; Minoura, N.; Kinoshita, T. *Colloid Polym. Sci.* **1995**, *273*, 1022.
(7) Seki, T.; Tamaki, T. *Chem. Lett.* **1993**, 1739.
(8) Seki, T.; Fukuda, R.; Yokoi, M.; Tamaki, T.; Ichimura, K. *Bull. Chem. Soc. Jpn.* **1996**, *69*, 2375.
(9) Steinem, C.; Janshoff, A.; Vollmer, M. S.; Ghadiri, M. R. *Langmuir* **1999**, *15*, 3956.
(10) Bullock, D. J. W.; Cumper, C. W. N.; Vogel, A. I. *J. Chem. Soc.* **1965**, 5316.
(11) Seki, T.; Sekizawa, H.; Morino, S.; Ichimura, K. *J. Phys. Chem. B* **1998**, *102*, 5313.
(12) Kago, K.; Fürst, M.; Matsuoka, H.; Yamaoka, H.; Seki, T. *Langmuir* **1999**, *15*, 2237.
(13) Seki, T.; Sekizawa, H.; Ichimura, K. *Polym. Commun.* **1997**, *38*, 725.
(14) Seki, T.; Sekizawa, H.; Ichimura, K. *Polym. J.* **1999**. *31*, 1079.
(15) Seki, T.; Tanaka, K.; Ichimura, K. *Macromolecules* **1997**, *30*, 6401.
(16) Related AFM studies dealing with the LB films composed of low molecular mass Az derivatives have also been reported: Vélez, M.; Mukhopadhyay, S.; Muzikante, I.; Matisova, G.; Vieira, *Langmuir* **1997**, *13*, 870. Wang, R.; Jiang, L.; Iyoda, T.; Tryk, A.; Hashimoto, K.; Fujishima, A. *Langmuir* **1996**, *12*, 2052.
(17) Matsumoto, M.; Miyazaki, D.; Tanaka, M.; Azumi, R.; Manda, E.; Kondo, Y.; Yoshno, N.; Tachibana, H. *J. Am. Chem. Soc.* **1998**, *120*, 1479.
(18) Seki, T.; Sakuragi, M.; Kawanishi, Y.; Suzuki, Y.; Tamaki, T.; Fukuda, R.; Ichimura, K. *Langmuir* **1993**, *9*, 211.
(19) Suzuki, M.; Aoyana, S.; Osada, T.; Nakano, A.; Suzuki, Y.; Takami, H.; Takenobu, T.; Yasutake, M. *J. Vac. Sci. Technol. A* **1996**, *14*, 1228.
(20) Beaglehole, D.; Radlinska, E. Z.; Ninham, B. W.; Christenson, H. K. *Phys. Rev. Lett.* **1991**, *66*, 2084.
(21) (a) Chen, Y.-L.; Israelachivili, J. N. *J. Phys. Chem.* **1992**, *96*, 7752. (b) Chen, Y. L. E.; Gee, M. L.; Helm, C. A.; Israelachvili, J. N.; McGuiggan, M. M. *J. Phys. Chem.* **1989**, *93*, 7057.
(22) Shiku, H.; Dunn, R. S. *J. Phys. Chem. B* **1998**, *102*, 3791.
(23) Rädler, J.; Strey, H.; Sackmann, E. *Langmuir* **1995**, *11*, 4539.
(24) Kumaki, J.; Nishikawa, Y.; Hashimoto, T. *J. Am. Chem. Soc.* **1996**, *119*, 3321.
(25) Shimomura, M.; Ando, R.; Kunitake, T. *Ber. Bunsen-Ges. Phys. Chem.* **1983**, *87*, 1134.
(26) Seki, T.; Kojima, J.; Ichimura, K. *J. Phys. Chem. B* **1999**, *103*, 10338.
(27) Frank, H. S.; Evans, M. W. *J. Chem. Phys.* **1945**, *13*, 507.
(28) Frank, F. S. *Faraday Symp. Chem. Soc.* **1982**, *17*, 7.
(29) Du, Quan.; Freysz.; Ahen, Y. R. *Science* **1994**, *264*, 826.
(30) Rochon, P.; Batalla, B.; Natansohn, A. *Appl. Phys. Lett.* **1995**, *66*, 136.
(31) Kim, D. Y.; Li, L.; Kumar, J.; Tripathy, S. K. *Appl. Phys. Lett.* **1995**, *66*, 1166.
(32) Ramanujam, P. S.; Holme, N. C. R.; Hvilsted, S. *Appl. Phys. Lett.* **1996**, *70*, 1518.
(33) Mendonça C. R.; Dhanabalan, A.; Balogh, D. T.; Misoguti, L.; dos Santos, Jr., D. S.; Pereira-da-Silva, M. A.; Giacometti, J. A.; Zilio, A. C.; Oliveira, O. N., Jr. *Macromolecules* **1999**, *32*, 1493.

MA991439I